CHAPTER 3

EXPERIMENTAL FAN BLADE DAMAGE SIMULATOR

As discussed in Chapter 1, it became clear at an early stage that it would be necessary to design and build an experimental test structure to facilitate the development of a damage identification technique. Cost and safety aspects make it impractical to develop such a technique on a fan in industry. The design and construction of the EFBDS from scratch took time, effort and a large amount of the available funds, but provided an excellent tool for the development of a damage identification technique. There would also not have been any way to know exactly what was required for a successful identification to be done. As mentioned in Chapter 1, a scanning laser vibrometer would be an ideal sensor, the cost of around 80 000 US $ was prohibitive however.

3.1 Design issues

In order for a technique, that can be used on fans such as FD fans, to be developed, the most important design aspect would be that results obtained from the experimental fan must be representative of FD fans. The EFBDS had to comply with the following specifications:

- Only ambient agitation should be used to excite the system.
- The blades should be attached to the structure in a similar way as that used on the FD fans.
- Variable speed should be available to proof that the technique works at any rotational speed. The EFBDS is roughly one fourth the size of an ID fan and the dynamics of blades change due to centrifugal acceleration. Different dynamics can be simulated by using different rotational speeds.
- The fan blades should have roughly the same aspect ratio as the existing blades.
- Should provide for growth in future research.

It was recognised at an early stage that it would not be possible to develop a damage detection technique and implement it on the actual structure within the time con-

straints of a masters degree. For this reason the simulator was given a modular design to facilitate further research.

3.2 Concepts and selection

3.2.1 Blade attachment

One of the most important aspects of the axial flow fans used at Majuba are the variable pitch blades used. Because of this arrangement, the hub is not a simple construction and takes up a relatively large percentage of the total diameter. Various methods for attaching blades with variable pitch were looked at. The most important and practical concepts are discussed below.

Wedge blocks

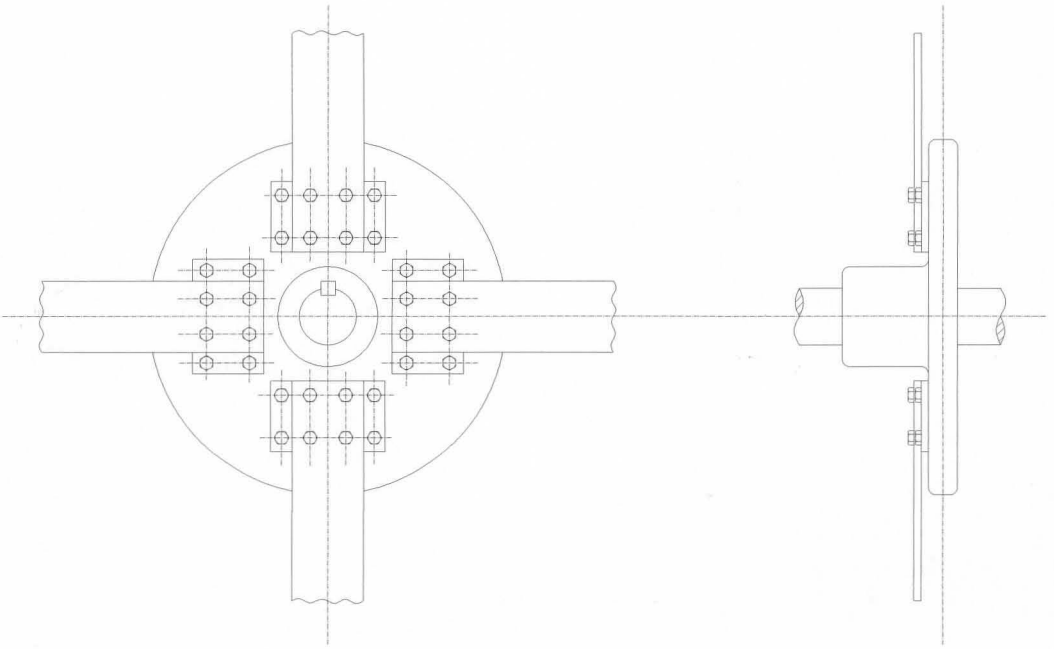

Figure 3.1: Wedge block schematic assembly drawing

The first method considered for adjusting the pitch of the blade made use of different wedge blocks. Each block would then represent a specific pitch. A schematic representation of the hub- and blade interface can be seen in Figure 3.1.

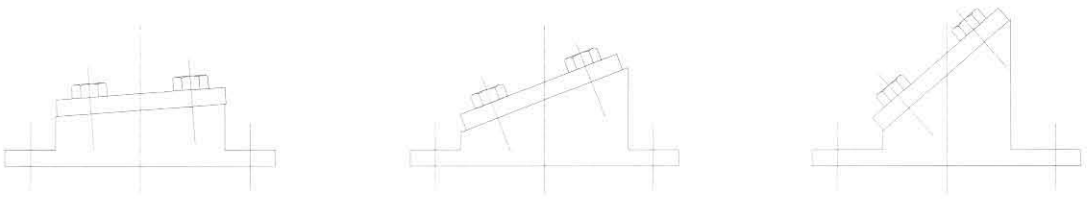

Figure 3.2: Different pitch angle configurations for the wedge block concept

Examples of the different wedge blocks that would be required can be seen in Figure 3.2.

Advantages of this concept was:

- Simple construction and machining.
- Relatively simple to change the pitch.
- All blades will have the same pitch angle.

Disadvantages was:

- A whole range of wedge blocks needed to be manufactured.
- Limited number of pitch angles available.
- Due to the space the wedge blocks occupied, the number of blades would probably have been restricted to four at most.
- The shear forces on the bolts that attached the blade to the hub may result in inaccurate frequency measurements at different fan speeds. Furthermore it did not represent the actual fan blades well.

Clamped blades

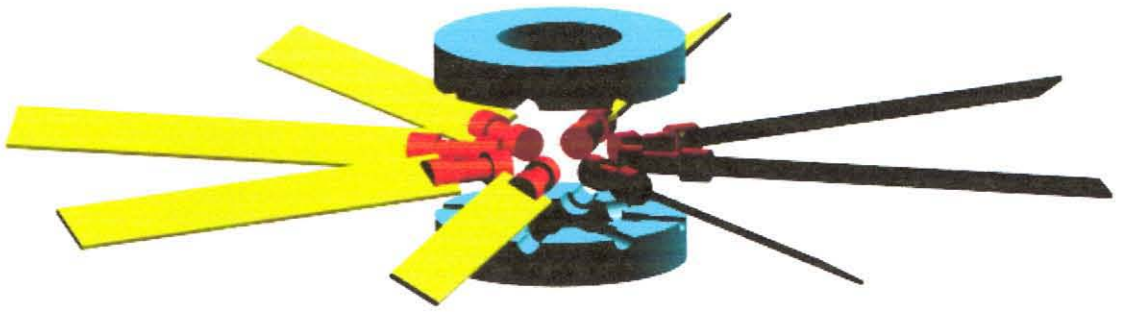

Figure 3.3: Clamped blades schematic concept drawing

To get around the problems of the wedge block concepts, the next concept looked at, was optimised for using the minimum space to hold blades, while offering a very wide range of pitch angles. A schematic three-dimensional representation of this concept can be seen in Figure 3.3. Some sort of indexing mechanism would off-course have to be employed to ensure that all the blades were at the same pitch for a particular measurement.

Advantages:

- More compact, can accommodate more blades if necessary.
- The blade attachment can be made to represent the actual fan blades more accurately.

Disadvantages:

- Very difficult to assemble and machine this concept.
- Some sort of an indexing mechanism would have been necessary to ensure the blades were all at the same pitch.

This concept presented a much more realistic approach for the fan blade damage simulator. The final development model was therefore an extension of this concept.

Inserted blades

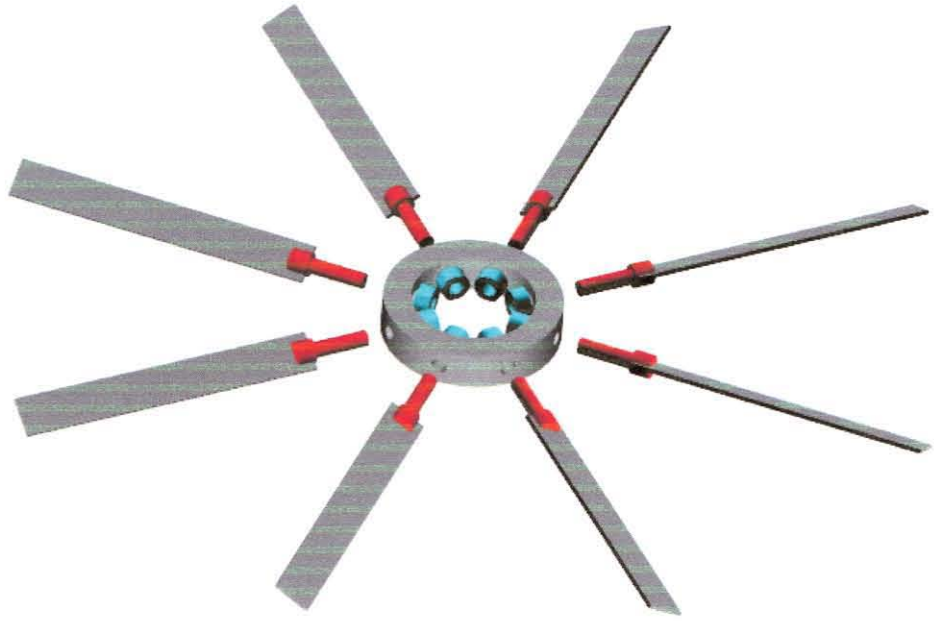

Figure 3.4: Inserted blades concepts

By keeping the blade seat interface as simple as possible to manufacture without loosing the advantages of the above concept, a concept using a solid ring with inserted blades was developed.

Clearly an indexing mechanism would also be needed for this interface. Since the blades can be inserted one at a time, this should not be a big problem.

Advantages:

- Compact, can accommodate more blades as necessary.
- Very close to the method used to fix the blades on the FD fan at Majuba.
- Relatively easy to change the pitch of the blades.
- Machining and assembly easier than clamped blades concept.

Disadvantages:

- Indexing mechanism will be necessary.
- All the force due to centrifugal acceleration has to be carried by the bolt and nut.

In the end this concept was developed into a final design for the interface between the blades and the hub. The final design can be seen in the section 3.3. of this chapter.

3.2.2 Drive design

To make it possible for the fan to be tested in an easily accessible location, it was decided not to use three-phase power. As a result the choice of a speed controlled electrical motor was limited to around 1.5 kW. More detail on the electric motor and speed control unit as well as the reasons for these choices follow in the next section.

The model was planned to be about a quarter scale model. To check whether the 1.5 kW motor would be adequate a simple calculation was done to calculate the amount of power 8 blades rotating at around 750 r.p.m. would absorb.

The following assumptions were made:

- Force on the blade was only due to the conservation of momentum
- Since air leak around the edges of the blade and a component flows in a radial direction along the blade the force was taken as around 60% of the computed force. This Figure corresponds to the efficiency of a fan with straight, simple blades (Osborne, (1977)).

- Compressibility of air was not taken into account.
- Blades do not influence one another.

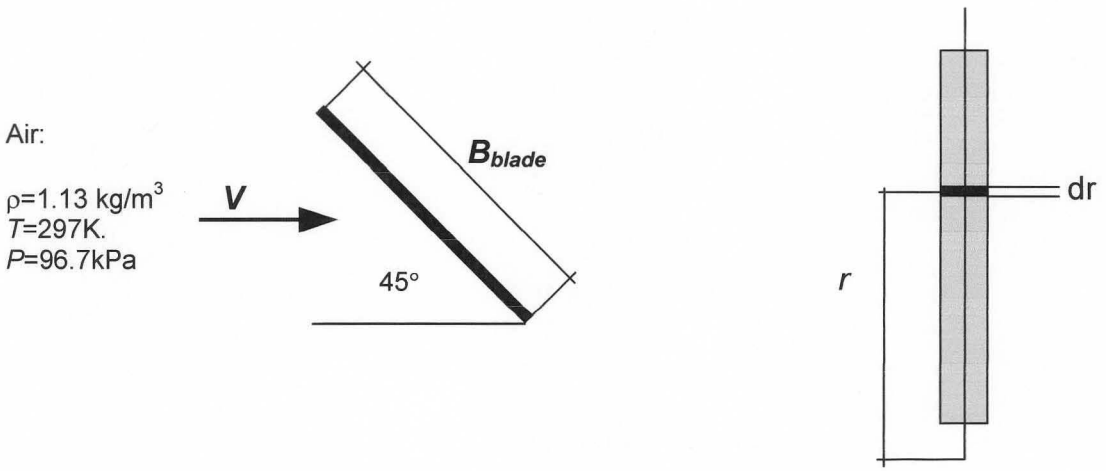

Figure 3.5: Schematic of simple blade moving through air

With reference to Figure 3.5 the mass flow of air was calculated as

$$\begin{aligned} M_{air} &= \rho A v \\ &= \rho \omega r B_{Blade} \sin 45^{o} \, dr \end{aligned} \tag{3.1}$$

$$\rho = 1.13 kg / m^{3}$$
$$A = (B_{blade}) \sin(45^{o}) dr$$
$$v = \omega \cdot r$$

The force acting on a finite section of the blade *dr* can then be calculated as

$$\begin{aligned} F_{Blade} &= M_{air} v \eta \\ &= \eta \rho \omega^{2} r^{2} B_{Blade} \sin 45^{o} \, dr \end{aligned} \tag{3.2}$$

The total moment on the shaft due to a single blade can then be calculated as

$$\begin{aligned} M_{shaft} &= F_{Blade} d \\ &= \eta \rho \omega^{2} r^{2} B_{Blade} \sin 45^{o} \, dr \int_{\text{Blade root radius}}^{\text{Blade tip radius}} r^{3} dr \end{aligned} \tag{3.3}$$

The power absorbed by a blade can then be calculated at 750 r.p.m. (ω=78.54 rad/s)

$$\begin{aligned} P_{Blade} &= M_{blade}\omega \\ &= \eta\rho\omega^3 B_{Blade} \sin 45^o \left[\frac{r^4}{4}\Big|_{0.15}^{0.485}\right] \\ &= 159W \,/\, blade \end{aligned} \qquad \textbf{(3.4)}$$

For eight blades this equates to 1.253 kW. A 1.5 kW motor would therefore be adequate. For reasons of simplicity and flexibility it was decided to use a belt drive. The main reasons were:

- The frame design was simplified since alignment of the motor with the shaft of the fan was not as important as it would have been with an inline shaft connection.
- The speed ratio between the motor (1450 r.p.m.) and the fan (750 r.p.m.) can easily be adjusted by using different pulley sizes.
- Centre of gravity of the structure is lower and a more sTable structure was the result.

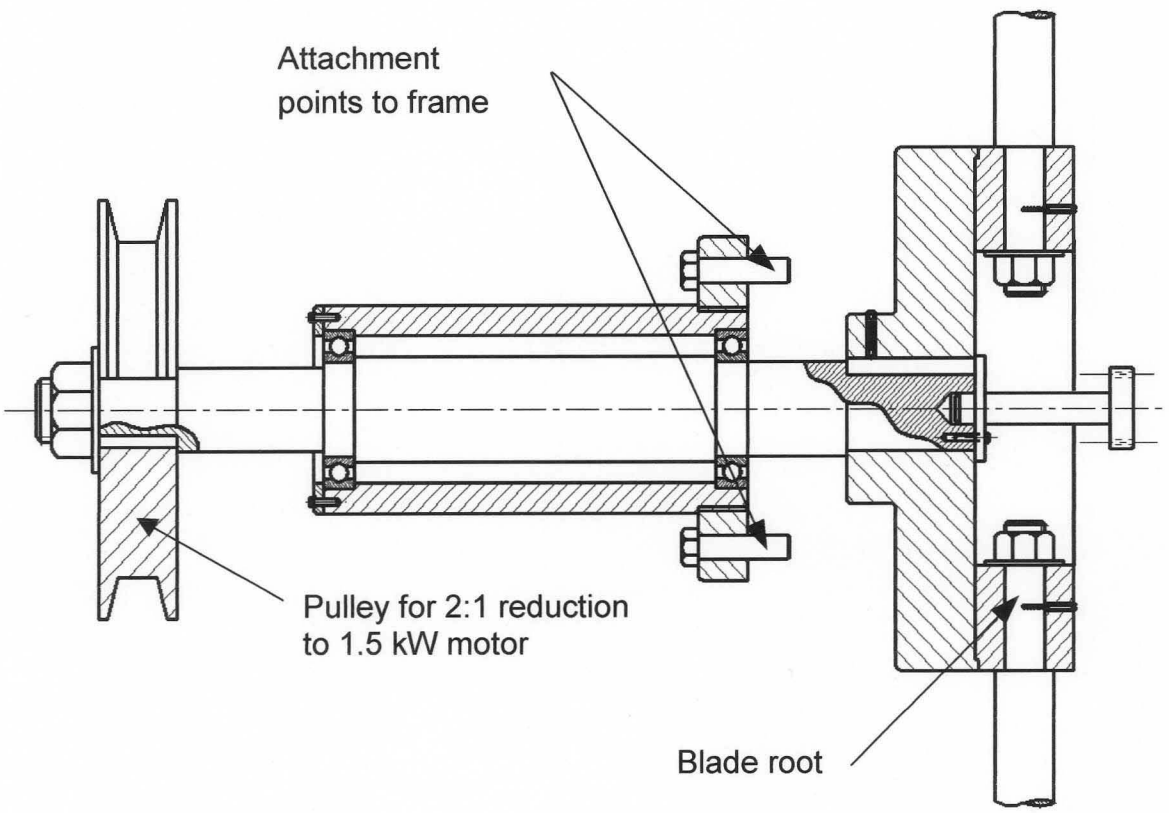

Figure 3.6: Final concept configuration before design refinements had been implemented

The fan belt- and bearing design was done according to the manufacturer's catalogues.

3.2.3 Final design

With the general layout of the fan and the methods for attaching blades decided on, various small changes had to be made to facilitate the manufacturing of the components. A schematic representation of experimental fan blade damage simulator can be seen in Figure 3.7.

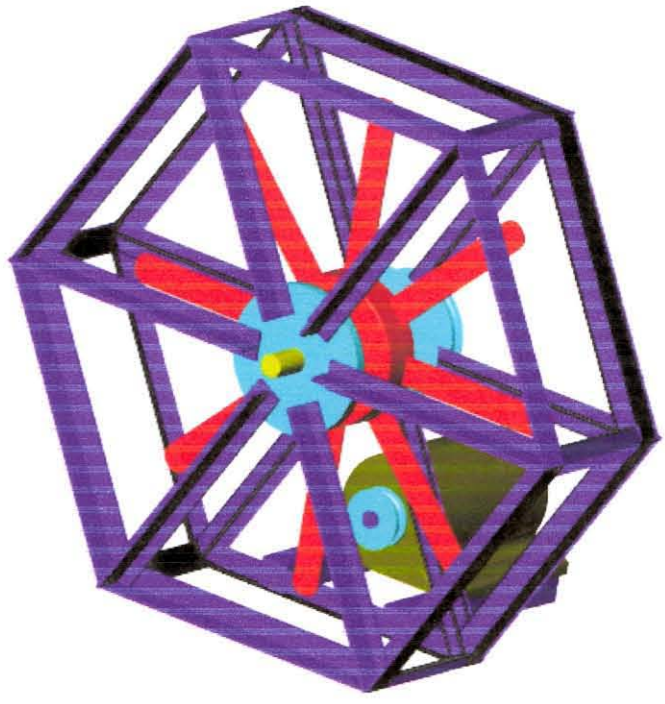

Figure 3.7: Schematic drawing of the final design of the fan

Most of the detailed manufacturing drawings are not included in this thesis since it had no real relevance on the outcome of the experiments. The blade seats and attachment to the hub are of some importance however and is shown in Figure 3.8 and 3.9.

With reference to Appendix B, it can be seen that the interface decided on was very similar to the actual fan found at the Majuba power plant. Because of the ability to change the pitch of the blade, the stiffness of the rotational axis around which the pitch was adjusted is not as high as the stiffness in the translation directions.

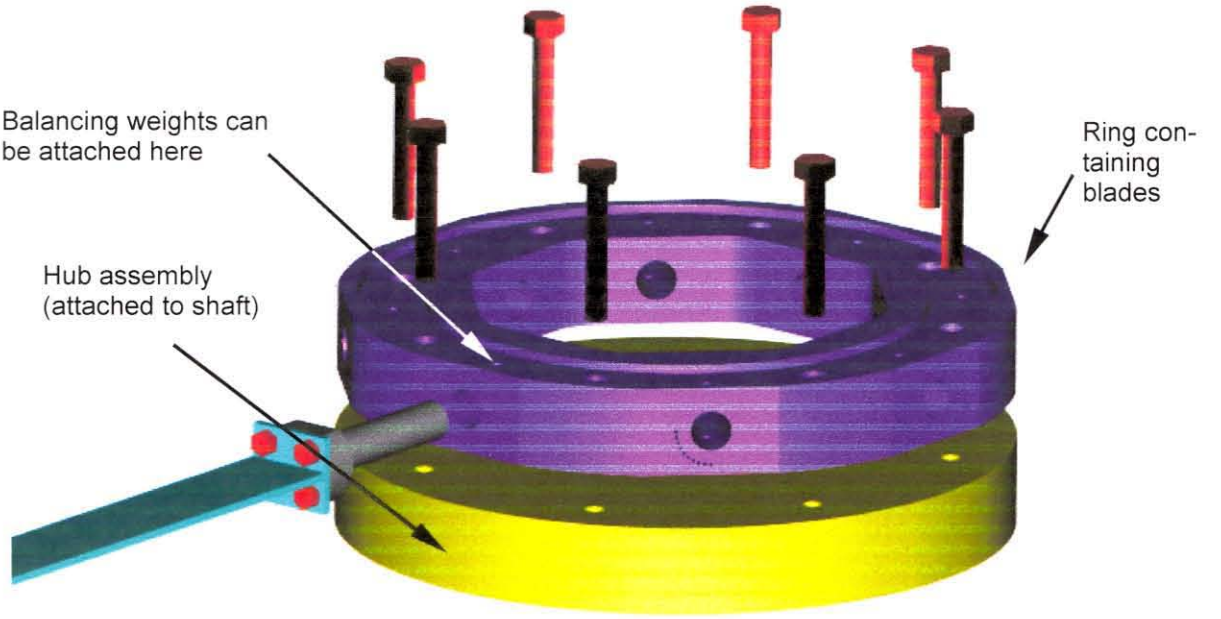

Figure 3.8: 3D representation of blade, hub interface

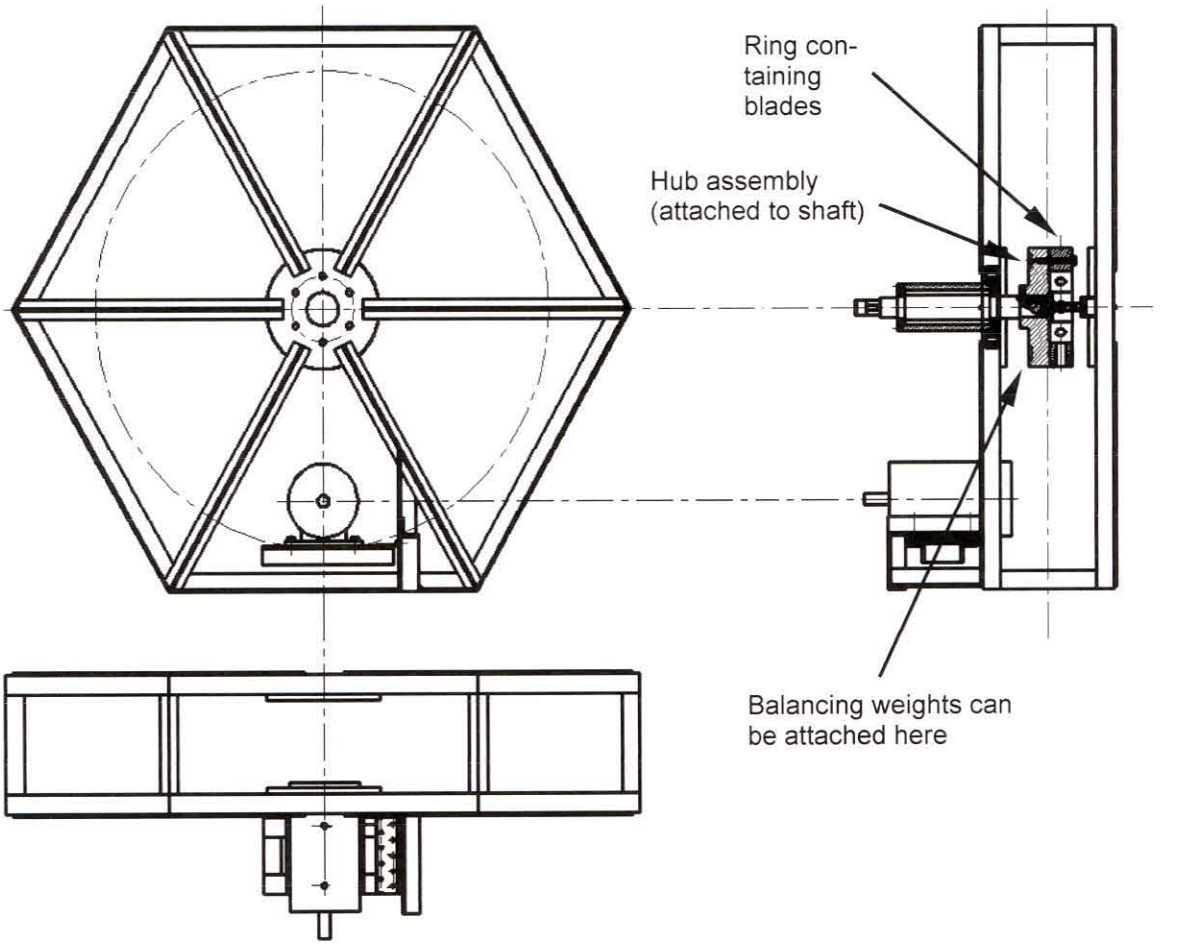

Figure 3.9: Assembled drawing (Blades excluded)

3.3 Manufactured fan blade damage simulator

As mentioned earlier in this chapter, the decision to install the EFBDS in an easily accessible location limited the power supply to single phase 220 V. While DC motors with a 1.5 kW rating do exist and excellent speed control can be applied to the motors, the total cost was approximately three times higher than an induction motor with an electronic speed control unit. The specifications for the speed controller can be seen in Table 3.1. The speed controller can run of a single phase 220 V supply. By varying the output frequency of the three-phases provided by the controller, the rotational speed of the induction motor can be selected.

The speed control unit used to control the three phase 1.5 kW electric motor can be seen in Figure 3.15.

Table 3.1: Specifications of speed controller

AC Tech Variable Speed AC Drive SF 100 series	
Storage Temperature	-20°C to 70°C
Ambient Operating Temperature	0°C to 50°C
Ambient Humidity	< 95% (non-condensing)
Maximum Altitude	3300ft (1000m) above sea level
Input Line Voltages	208/240 Vac
Input Voltage Tolerance	+10%, -15%
Input Frequency Tolerance	48Hz to 62Hz
Output Wave Form	Sine Coded PWM
Output Frequency	0-240Hz
Service Factor	1.00
Efficiency	Up to 98%
Power Factor	0.96 or better
Overload Current Capacity	150% for 60 seconds, 180% for 30 seconds.
Speed Reference Follower	0-10 VDC, 4-20mA
Control Voltage	15 VDC
Power Supply for Auxiliary Relays	50 mA @ 12 VDC
Analog Outputs	0-10 VDC proportional to frequency or load
Digital Outputs	Open collector outputs: 50 mA @ 30 VDC

Before measurements could be taken on the EFBDS, the ring containing the blade seats had to be aligned with the hub assembly (see Figures 3.8 and 3.9). Balancing surfaces provided on the hub assembly proved unnecessary as the first rotational frequency fell well below the first natural frequency and was filtered out using a high pass filter. In addition, the unbalance was relatively little and did not appear to influence measurements significantly.

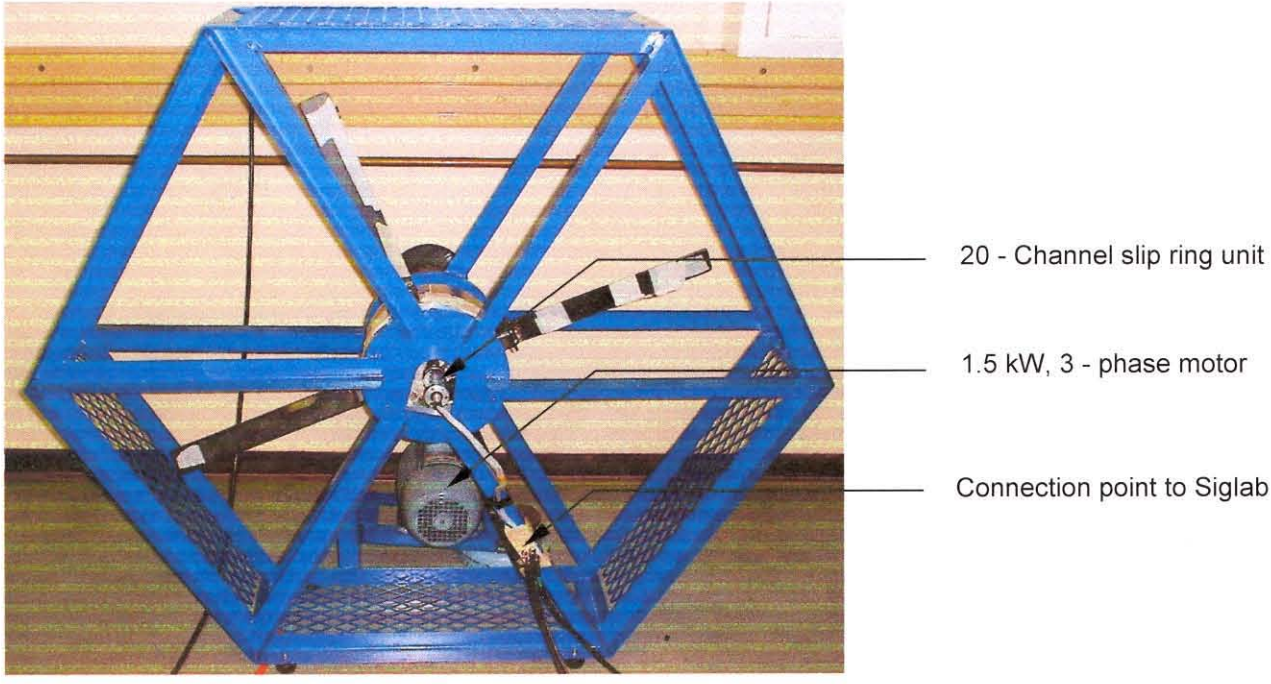

Figure 3.10: Experimental fan blade damage simulator

The completed experimental fan blade damage simulator can be seen in Figures 3.10 through 3.14.

Figure 3.11: Side view

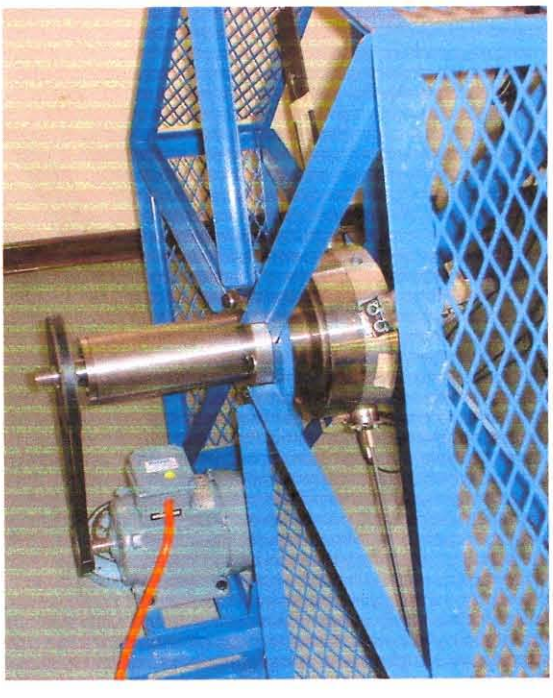

Figure 3.12: Rear view

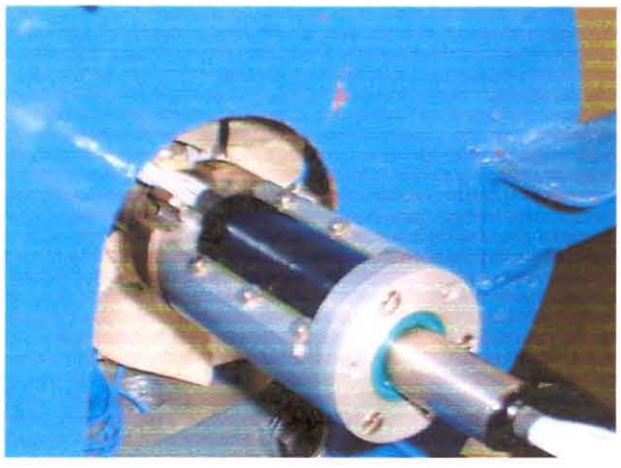

Figure 3.13: Close up of 20 – channel slip ring unit

Figure 3.14: Close up of the blade seat and attachment

The method with which the blades were attached to the blade seats can clearly be seen in Figure 3.14. This was a good simulation of the way in which the actual fan blades at Majuba are attached. Figure 3.13 show the 20–channel slip ring unit. Specifications can be seen in Table 3.2. The unit made use of gold alloy brushes and slip rings to transfer power to the various transducers and measure the output.

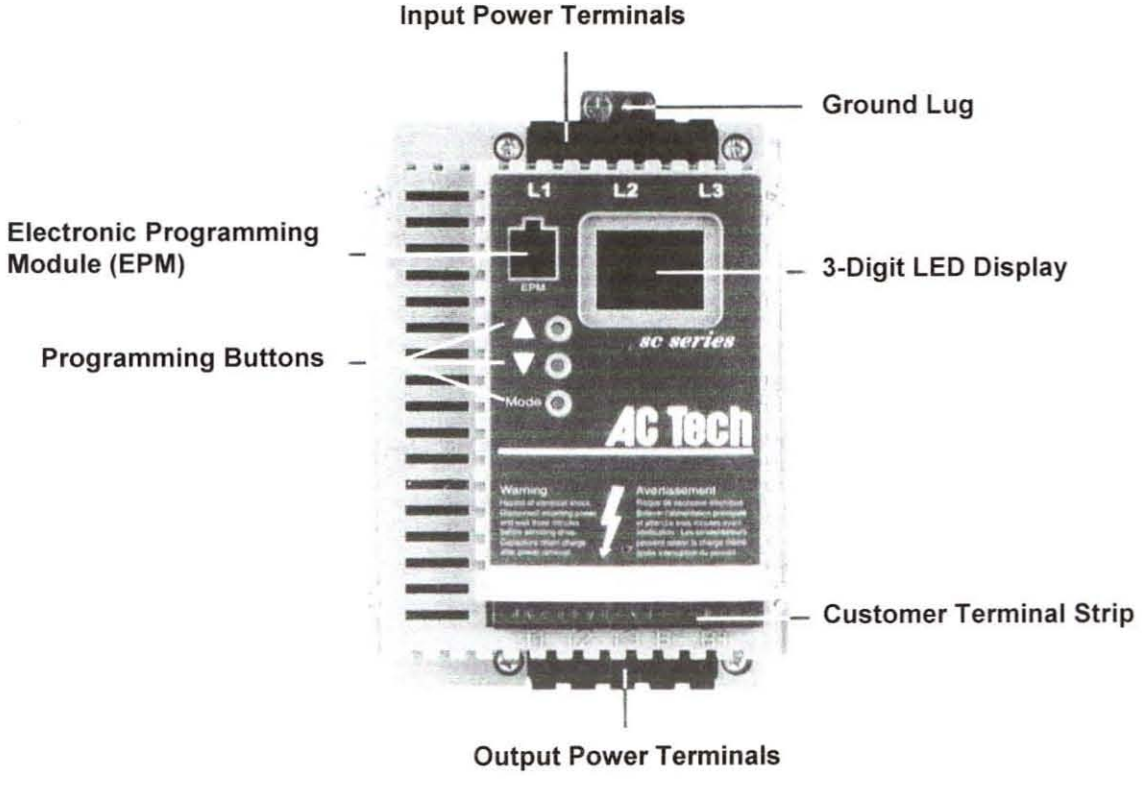

Figure 3.15: The speed controller used for the 1.5 kW 3-phase motor

Table 3.2: Specifications of the 20 – channel slipring unit

C-series slip rings (C-20)	
Current (continuous)	2.6A per circuit
Current (peak)	4A per circuit for 10 seconds
Voltage	200 VDC
Insulation resistance	> 200 MΩ at 500 VDC
Contact resistance	< 20 mΩ
Recommended maximum speed	600 r.p.m.
Life	12 million revolutions minimum
Rings	Hard gold plated.
Brushes	Gold alloy covered spring steel.
Wire	Teflon coated
Sealing	IP:64
Surface treatment	Clear anodize

Permission was granted by the manufacturers to use the unit at 750 r.p.m. and they claimed that speeds of up to 1200 r.p.m. should not cause a significant increase in resistance or wear. The minimum operational time expected can thus be calculated as approximately 260 hours. The brushes and rings can be re-plated with gold alloy should it be required.

3.4 Conclusion

The EFBDS performed very well throughout the experimental testing phase and due to the modular designs, further development should not be a problem. The experimental results obtained are presented in the next chapter.